

Nanoscale

Accepted Manuscript



This is an *Accepted Manuscript*, which has been through the Royal Society of Chemistry peer review process and has been accepted for publication.

Accepted Manuscripts are published online shortly after acceptance, before technical editing, formatting and proof reading. Using this free service, authors can make their results available to the community, in citable form, before we publish the edited article. We will replace this *Accepted Manuscript* with the edited and formatted *Advance Article* as soon as it is available.

You can find more information about *Accepted Manuscripts* in the [Information for Authors](#).

Please note that technical editing may introduce minor changes to the text and/or graphics, which may alter content. The journal's standard [Terms & Conditions](#) and the [Ethical guidelines](#) still apply. In no event shall the Royal Society of Chemistry be held responsible for any errors or omissions in this *Accepted Manuscript* or any consequences arising from the use of any information it contains.

Cite this: DOI: 10.1039/c0xx00000x

www.rsc.org/xxxxxx

ARTICLE TYPE

One-pot synthesis of ultralong coaxial Au@Pt nanocables with numerous highly catalytically active perpendicular twinning boundaries and Au@Pt core-shell bead structures

Jisun Yoon,^a Hionsuck Baik,^{* b} Sangmin Lee,^c Seong Jung Kwon,^{* c} and Kwangyeol Lee^{*a}⁵ Received (in XXX, XXX) Xth XXXXXXXXX 20XX, Accepted Xth XXXXXXXXX 20XX

DOI: 10.1039/b000000x

Ultralong coaxial Au@Pt nanocable prepared by one-pot synthesis exhibits an excellent electrocatalytic activity due to structural features of 1) numerous twinning boundaries and 2) lattice mismatch between core and shell.

Core-shell nanoparticles has led to a number of important technological breakthroughs in catalysis, optics, and electronics.¹⁻⁷ For example, core-shell Au@Pt nanoparticles with lattice mismatch between core and shell have shown much improved catalytic performance over Pt nanoparticles.⁸⁻¹⁰ A number of core-shell nanoparticles¹⁻¹⁰ (metal, quantum dot, metal oxide) have been conveniently prepared by epitaxial growth of new phase on existing nanoparticles.¹¹⁻¹³ On the other hand, one-dimensional (1-D) nanostructures such as semiconductor nanowires of various compositions¹⁴⁻¹⁸ and carbon nanotubes^{19,20} have attracted a great interest due to their unique chemical and physical properties,¹⁴⁻²⁰ and bimetallic coaxial nanocable structures are also expected to exhibit novel catalytic applications.²¹⁻²³ Conceptually, coaxial bimetallic nanocables can be prepared by growing heterometal on the existing metallic nanowire. However, such examples are utterly rare plausibly due to the difficulty in the conformal coating of metallic nanowires without compromising the structural integrity of the template nanowires, especially when the nanowire diameter is less than 5 nm. We have recently found that the surface binding moiety CO, which exhibits a strong affinity to Pt atoms, could confine Pt component on the surface in heteronanostructure.²⁴ By utilizing this phenomenon, we could stabilize the kinetically favored but unstable structure of ultrathin Au nanowire even at high temperatures by *in situ* surface coating of Au nanowires with Pt layer. Herein, we demonstrate the successful one-pot preparation of ultra-long AuPt alloy nanowires and coaxial Au@Pt nanocable by taking advantage of the differential CO binding affinities between Pt and Au. We also report the excellent electrocatalytic

property of Au@Pt nanocable toward methanol oxidation reaction.

The composition in the alloy nanoparticles can be dynamically controlled by the nature of surface binding moieties. For example, the alloy RhPd nanoparticle changes the composition to form Pd@Rh and Rh@Pd according to the bound oxidizing or reducing gas molecules.²⁵ Therefore, a core-shell Au@Pt nanostructure might be prepared from a random alloy AuPt nanostructure in the presence of CO, because Pt atoms with a stronger metal-CO strength would be likely found on the surface.²⁶ We discovered that co-decomposition of Au and Pt precursors in oleylamine in the presence of CO at 90 °C leads to the formation of self-catalytic Au nanoparticles and halving of these Au nanoparticles, fast Au nanowire growth between the two halved Au nanoparticle heads, followed by surface-confined deposition of Pt on the mostly Au-based nanowires, resulting in the formation of structure-fortified ultralong (> 10 μm) AuPt nanowires. Subsequent heating of the AuPt nanowires at 210 °C causes further surface-confined Pt deposition on the nanowire leading to unprecedented ultralong and ultrathin Au@Pt coaxial nanocables, which exhibit numerous twinning boundaries perpendicular to the nanowire growth axis and Au@Pt core-shell beads with lattice mismatch between core and shell.

A slurry of Pt(acac)₂ (0.1 mmol, Aldrich, 97%), HAuCl₄·xH₂O (0.1 mmol, Aldrich, 99.999%) and oleylamine 6 mL (Aldrich, 70%) was prepared in a two-neck bottom flask (50 mL) with a magnetic stirring and was placed under CO atmosphere. The reaction mixture was heated up to 90 °C at a heating rate of 3 °C/min, and kept at that temperature for 6 h to form AuPt nanowires. The reaction mixture was subsequently heated to 210 °C at a heating rate of 8 °C/min and kept at that temperature for 1 min under CO to give ultralong thin Au@Pt coaxial nanocables. The transmission electron microscopy (TEM), high resolution TEM (HRTEM) and scanning transmission electron microscopy (STEM) images of Au@Pt coaxial nanocables are shown in Fig. 1. As judged from TEM images in Fig. 1a, b, a very small diameter of 2~3 nm and a very long length (> 1 μm) are consistently found for all the nanowires. Higher magnification image of the nanowire reveals the presence of numerous small bead-like structures with diameters of 3~4 nm. Elemental mapping of the nanostructures shows a very interesting structural feature, namely Au@Pt core-shell nanocable structure. The Au

^a Department of Chemistry and Research Institute for Natural Sciences, Korea University, Seoul 136-701 (Korea). Tel: +82-2-3290-3139; E-mail: kylee1@korea.ac.kr

^b Korea Basic Science Institute (KBSI), Seoul 136-713 (Korea) Tel: +82-2-6943-4117; E-mail: baikhs@kbsi.re.kr

^c Department of Chemistry, Konkuk University, Seoul, 143-701 (Korea). Tel: +82-2-450-3629; E-mail: sjkwon@konkuk.ac.kr

† Electronic Supplementary Information (ESI) available.

mapping data shows the presence of very thin Au nanowires with the uniform diameter of ~ 2 nm. Pt phase is found confined to the surface of the Au nanowire, and the bead-like morphology is evidently caused by the localized growth of numerous Pt crystallites. Therefore, the prepared nanostructure can be described as a thin Au nanowire placed in a very thin Pt sheath, which is in turn decorated by numerous Pt beads. HRTEM image of the nanocables in Fig. 1g shows the presence of numerous twinning boundaries (\sim one twinning site per 2 nm of nanocable length), which are perpendicular to the Au nanowire growth direction of $\langle 111 \rangle$. A similar perpendicular twinning has been documented for Au nanowires prepared by different routes.²⁷

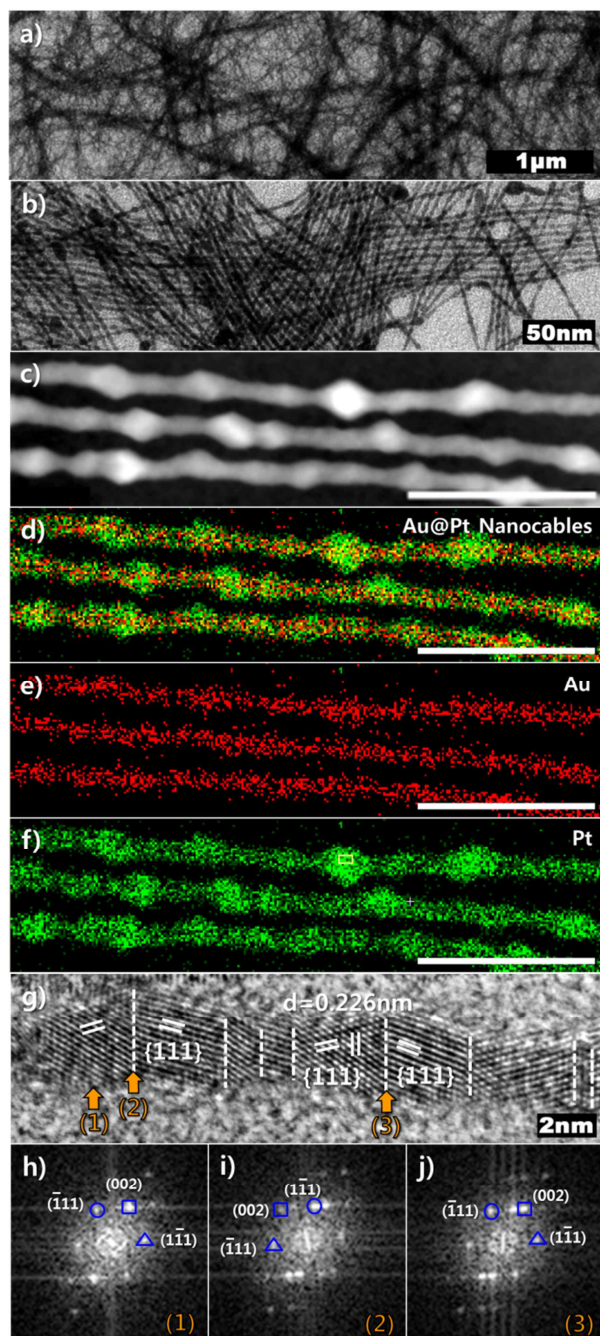


Fig. 1 (a,b) TEM images and (c) STEM image and (d-f) elemental mapping of Au@Pt nanowires. The scale bars in (c-f) are 20 nm. (g) HRTEM image of a (2–3 nm) \times (2–4) μ m Au@Pt nanocable. The white

dotted lines in (g) indicate the twin boundaries. The corresponding FFT patterns with zone axis of $\langle 110 \rangle$ are shown for (h) a single crystal domain and for (i,j) twin boundaries.

While $\{100\}$ Pt is preferentially stabilized under CO atmosphere,^{28–31} the exposed Pt facets on the Au nanowire are predominantly $\{111\}$ Pt, plausibly due to the effect of underlying Au crystal facet. Furthermore, the localization of Pt, thus, the formation of Au@Pt beads, always occurs on the twinning boundary. The highly energetic nature of twinning boundary requires further surface energy minimization and this can be accomplished by growth of larger nanocrystallites. This phenomenon is greatly beneficial to the catalytic activity of Pt-based catalyst, because the twinned crystal structure of Au would be epitaxially transferred to the Pt shell; twinned Pt nanostructure is expected to be catalytically highly active.³¹ In short, the coaxial cable nanostructure contains numerous catalytically active nanostructures of both Au@Pt core-shell structure and twinned Pt surfaces.

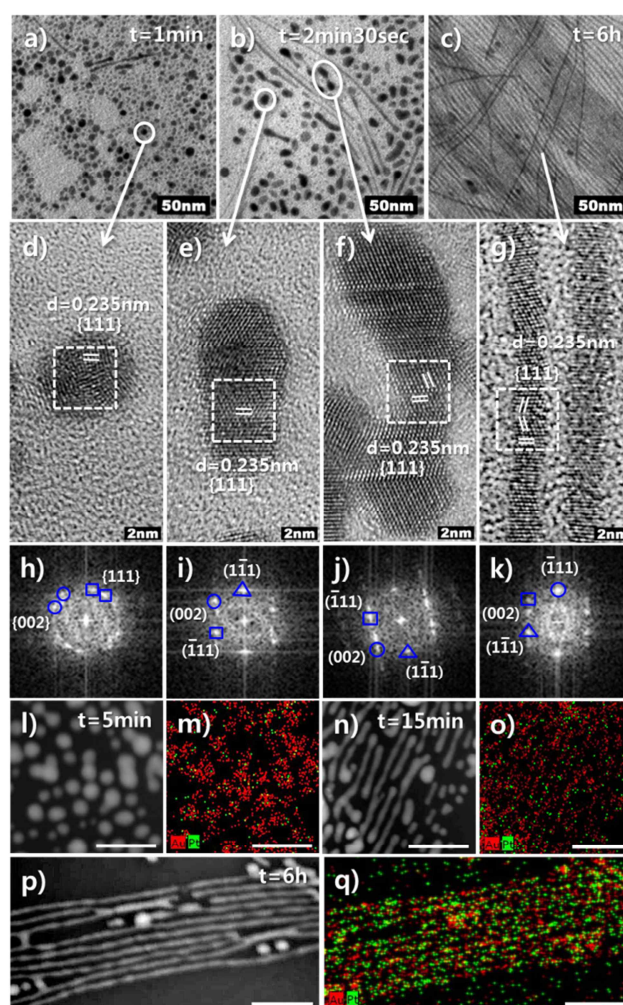


Fig. 2 TEM images of intermediates for the formation of Pt-doped Au nanowires at 90 °C after (a) 1 min, (b) 2 min 30 sec, (c) 6 h. HR-TEM images of various intermediate shapes of (d) a sphere, (e) a peanut, (f) a dumbbell, and (g) a wire. (h–k) The corresponding FFT patterns of the each structure with zone axis of $\langle 110 \rangle$. (l, n, p) STEM images and (m, o, q) elemental mapping of Pt-doped Au nanostructures at different reaction time of (l,m) 5 min, (n,o) 15 min, (p,q) 6 h. (l–o) When nanowires of early stage, thus not much doped by Pt, are exposed to the electron beam, structural instability of nanowires was observed to form small nanoparticles.

In order to understand the detailed growth mechanism, we obtained the temporal images of the reaction mixture aliquots as shown in Fig. 2. Initially irregular shaped nanoparticles are observed. (Fig. 2a) Interestingly, many of the initially formed Au nanoparticles became halved to form dumbbell shapes, namely, two large heads connected by a thin nanorod. (Fig. 2b) Elemental mapping shows that both irregular shaped nanoparticles and dumbbell shaped nanostructures are mainly composed of Au atoms; only a marginal fraction of Pt, less than 2%, is observed for these structures. It is noteworthy that Au nanowire growth speeds are utterly non-uniform among initially formed self-catalytic Au nanoparticles. Also, once initiated, the growth of Au-based thin nanowires seems to proceed at enormous speed. As shown in Fig. S5a, nanowire length of 2–3 μm can be obtained even within 1 min.

Interestingly, as shown in Fig. 2d-g, twinning is a conspicuous feature of all Au nanostructures. Initially formed irregular shaped nanoparticles exhibit multiply twinned structures. Halving of the nanoparticles and the growth of thin nanorod between them seems to indicate that the nanorod growth occurs via inserting the incoming Au atoms into the $\{111\}$ Au twinning boundary. The explosive and non-uniform growth of nanowire is also consistent with the presence of multiple growth sites. Once the Au nanorod with multiple perpendicular twinning boundaries is formed, the 1-D structure is elongated at very high speed to form ultralong Au nanowire, which easily exceeds the length up to 10 μm (Fig. 2g). Oriented attachment of small nanoparticles has been proposed as a plausible mechanism for the formation of various nanowires.^{27,32-34} Although oriented attachment of small Au nanocrystals could still lead to the fast growth of the nanowire, the temporal TEM images do not directly support this mechanism. The very fast growth of Au nanowire along $\langle 111 \rangle$ direction might lead to further formation of twinning sites in the nanowire, which in turn further speeds up the nanowire growth. The role of surface-confined Pt seems to lie in the structure stabilization of thin Au nanowires. Au nanowires can be formed even in the absence of Pt precursors. At the employed reaction temperature of 90 $^{\circ}\text{C}$, the ultrathin Au nanowires are easily deformed to spherical Au nanoparticles in the absence of added $\text{Pt}(\text{acac})_2$ (Fig. 3). Also, Au nanowires prepared by using only Au precursors are very unstable and broken easily to form Au droplets under focused TEM electron beam at 200 kV, while Pt-doped Au nanowires exhibit structural integrity under the same condition. It is noteworthy that the structural fortification of Au nanowire can be accomplished by only 2% Pt doping level, which is found for Au nanowires synthesized at 90 $^{\circ}\text{C}$ for 15 min (Fig. S6b). Prolonged heating of the reaction mixture at 90 $^{\circ}\text{C}$ for 6 h increases the Pt level to 20% (Fig. S6c). On the other hand, without employed CO, the formation of Pt-doped Au nanowires was not observed at 90 $^{\circ}\text{C}$; only spherical Au nanoparticles were formed under this condition (Fig. S7c). Obviously, the reduction of Pt and Au precursors was much facilitated by the reducing gas CO in our condition. Also, the fast nanowire formation condition assisted by CO obviously have resulted the multiple twinning in the nanowire, since slow reduction of the Au precursors would favor the formation of single crystalline nanostructures.³⁵ The aurophilic attachment of oleylamine to result in 1-D Au nanostructure has been well documented. For example, Au nanowires are formed from the reaction of $\text{HAuCl}_4 \cdot x\text{H}_2\text{O}$ and oleylamine under Ar gas for 4 days.³⁵ We also believe that the

presence of excess amount of oleylamine has contributed to accelerating the nanowire growth by greatly reducing the thermal decomposition temperature of both metal precursors.³⁶

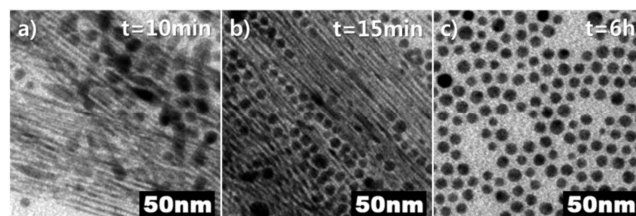


Fig. 3 TEM images of Au nanowires and nanoparticles synthesized with same condition for the formation Pt-doped Au nanowires without added $\text{Pt}(\text{acac})_2$. Gradual disappearance of Au nanowire is observed with prolonged heating, which was not observed in the presence of added Pt precursor. Therefore, the Pt-doping is utterly important in stabilizing the nanowire morphology under the reaction condition.

Once all the Au precursors are used up, the surface coating of Pt would be the major reaction process. Further elevating of the reaction temperature leads to the complete Pt deposition on the nanowire surface and localized Pt nanocrystallite growth on the highly energetic twinning boundary of Au nanowire to minimize surface energy. The schematic view of the nanowire growth and Au@Pt nanocable formation mechanism is depicted in Fig. 4.

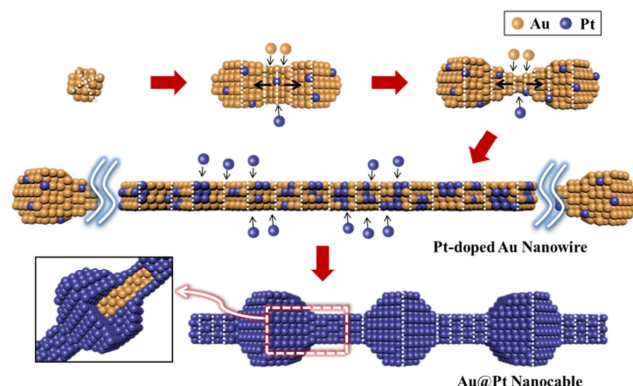


Fig. 4 Schematic view of the formation coaxial Au@Pt nanocables. White dotted lines indicate twinning boundaries.

The nanowire morphological control was investigated under different precursor ratios as shown in Fig. 5. The formation of nanowires was observed for the Au/Pt ratios ranging from 2/1 to 1/10, with the highest nanowire yield found at 1/1 (Fig. 5d, S8). With higher Au/Pt ratios, longer nanowire length was obtained. At high Au/Pt ratio of 2/1 and 1.5/1, large Au nanoparticles attached onto the nanowires are also observed, plausibly indicating the role of Pt in stabilizing Au nanowire morphology by suppressing the lateral Au growth. On the other hand, by increasing Pt component, the nanowire length was shortened and the bead-like structure became more evident. At high Pt precursor conditions, the catalytic Au heads might be over-coated by the Pt, leading to the suppression of Au nanowire growth, which necessitates Au atom insertion into the twinning interfaces. It should be mentioned that the necklace-like structures shown in Fig. 5a-5c are found only as minor products along with spherical Au@Pt core-shell nanoparticles under high Pt precursor conditions.

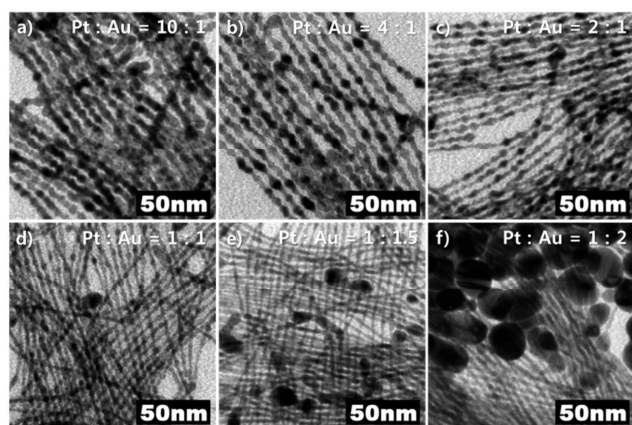


Fig. 5 TEM images of Au@Pt nanowires synthesized through using the different molar ratio of Pt(acac)₂ to HAuCl₄ · xH₂O.

Surface energy modulation of nanoparticles serves as a strategy to control catalytic selectivity as well as activity.^{12, 37, 38} Combining the core-shell structure and twinning could result in the surface energy elevation, leading to a great improvement in catalytic activity.²⁴ The coaxial Au@Pt nanocable exhibits numerous Au@Pt beads with surface energy elevating core-shell lattice mismatch and the Pt shells on the Au@Pt beads invariably show twinning boundary because of the epitaxial transfer of underlying twinned Au crystal structure. In order to assess the synergistic effect of Au core-Pt shell lattice mismatch and twinning interface on the Pt shell of Au@Pt coaxial nanocables on the catalytic performance, the electrocatalytic properties of Au@Pt nanocables toward methanol oxidation reaction (MOR) were examined and compared with other nanostructures (Fig. S10) reported in previous studies³¹ as shown in Fig. 6. Before the cyclic voltammograms (CVs) were obtained, the nanostructure modified electrodes were cleaned electrochemically by scanning the potential between 0.0 V (vs. NHE) and 1.6 V in 0.5 M H₂SO₄ solution.

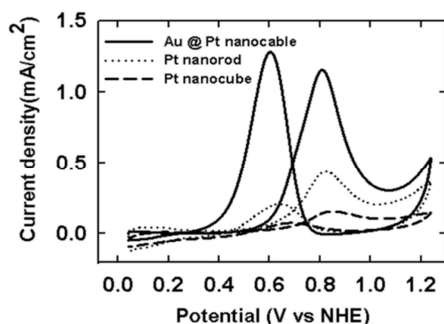


Fig. 6 Cyclic voltammograms of Pt nanostructures-modified glassy carbon electrodes (GCEs) in 0.5 M MeOH + 0.5 M H₂SO₄ electrolyte solution. Scan rate was 50 mV/s.

The current densities, the mass activity, and the electrochemically active surface areas (ECSA), which were determined by the hydrogen desorption method, are shown in Table. 1. The methanol oxidation peaks for the Au@Pt nanocable-modified GCE appeared at ~0.8 V in the forward and at ~0.6 V in the backward sweep. It is consistent with typical features of the methanol oxidation at Pt surface in previous literatures.³⁹

Nano structure	ECSA (m ² /g)	Forward scan		Backward scan	
		Current density (mA/cm ²)	Mass activity (mA/mg)	Current density (mA/cm ²)	Mass activity (mA/mg)
Au@Pt nanocable	75.0	1.15	866	1.28	961
Pt nanorod	13.8	0.43	59.7	0.37	50.7
Pt nanocube	13.9	0.16	21.5	0.15	20.8

Table. 1 Electrocatalytic properties of Pt nanostructures for MOR

The forward peak is due to the methanol oxidation, and the backward peak is responsible for the oxidation of adsorbed CO or CO-like species which are generated by incomplete methanol oxidation and are poisoning the active site of Pt.⁴⁰ As judged solely by the forward peak current (*i_F*)/backward peak current (*i_B*) ratio, the Au@Pt nanocable seems to be more affected by poisoning than Pt nanorod or Pt nanocube. The exact nature of poisoning species needs to be elucidated by further studies. Despite the low value of forward peak current (*i_F*)/backward peak current (*i_B*) ratio, however, the Au@Pt nanocable shows greatly improved electrocatalytic activity than the other previously reported nanostructures. We previously showed that the twinning in the Pt nanorod has roughly 3-fold enhancement over single crystalline {100} Pt nanocube. The twinned core-shell structure of Au@Pt nanocable exhibits catalytic activity 3 times higher than the five-fold twinned Pt nanorod and 10 times higher than the {100} Pt nanocube. Recently prepared ultrathin Pt multiply-twinned nanowire networks showed mass activities of 580 and 764 mA/mg for forward scan and backward scan respectively.⁴⁰ The introduction of structural element of core-shell mismatch into Au@Pt nanocable, in addition to the twinning property, leads even better catalytic activities of 866 and 961 mA/mg. Chronoamperometry (CA) experiments, performed at 0.84 V for the Au@Pt nanocable, demonstrated much better electrochemical stability of Au@Pt nanocable toward MOR over those of Pt nanorod or nanocube, plausibly due to the structural robustness (Fig. S11). Recent studies demonstrated the structural robustness of concave Pt structures and networked 3-D Pt structures during electrocatalytic applications.^{41,42} Therefore, it appears that the ultralong Au@Pt nanocables preserve the structural integrity during electrochemical applications by forming entangled 3-D nanostructures.

The electro-catalytic property of Au@Pt nanocable toward oxygen reduction reaction (ORR) was also investigated. (Fig. S12). Although the Au@Pt nanocable shows improvement in the ECSA and mass activity for the ORR over other nanostructures (Table. S1), the current density of Au@Pt nanocable was not improved from Pt nanocube and five-fold twinned Pt nanorod. The different tendency of the current density for ORR and MOR implies the active sites for these reactions are not identical, calling for further study to identify the active sites for ORR and MOR in order to design optimal nanocatalyst structures. It has been also reported that the different high energy structural feature of surface steps is beneficial to the MOR activity, while being indifferent to the ORR activity.⁴³

Conclusions

In summary, we have successfully demonstrated the one-pot synthesis of highly efficient electrocatalytic 1-D nanostructure of coaxial Au@Pt nanocable, which exhibits numerous twinning boundaries perpendicular to the nanowire growth direction as well as twinning boundary presenting Au@Pt core-shell beads on

the Au twinning boundaries. We believe that other related 1-D nanostructures could be synthesized by employing the same synthetic concept of synchronizing the nanowire growth and heteroepitaxial lateral growth. The co-localization of highly energetic structures of core-shell lattice mismatch and twinning boundary leads to synergistic improvement of electrocatalytic activity towards methanol oxidation reaction. Further composition and facet control of the coaxial cable nanostructure motif would lead to fine-tuning of the catalytic performance. Also, conducting metal-based 1-D nanostructures of this study are currently being investigated for the applications in sensors and flexible displays.

Acknowledgements

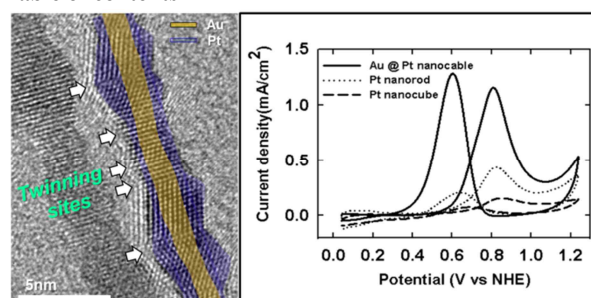
This work was supported by NRF-2013R1A2A2A 01015168, NRF 2010-0020209, NRF 2014M3A6B2, KBSI project T34520. We thank KBSI for allowing the usage of their HRTEM instruments.

Notes and references

- 1 S. Kim, B. Fisher, H. J. Eisler and M. Bawendi, *J. Am. Chem. Soc.*, 2003, **125**, 11466.
- 2 H. Kim, M. Achermann, L. P. Balet, J. A. Hollingsworth and V. I. Klimov, *J. Am. Chem. Soc.*, 2005, **127**, 544.
- 3 J. Zhang, F. H. B. Lima, M. H. Shao, K. Sasaki, J. X. Wang, J. Hanson and R. R. Adzic, *J. Phys. Chem. B*, 2005, **109**, 22701.
- 4 S. Alayoglu, A. U. Nilekar, M. Mavrikakis and B. Elchhorn, *Nat. Mater.*, 2008, **7**, 333.
- 5 V. Mazumder, M. Chi, K. L. More and S. Sun, *J. Am. Chem. Soc.*, 2010, **132**, 7848.
- 6 P. strasser, S. Koh, T. Anniyev, J. Greeley, K. More, C. Yu, Z. Liu, S. Kaya, D. Nordlund, H. Ogasawara, M. F. Toney and A. Nilsson, *Nat. Chem.*, 2010, **2**, 454.
- 7 D. Wang, H. L. Xin, R. Hovden, H. Wang, Y. Yu, D. A. Muller, F. J. Disalvo and H. D. Abruna, *Nat. Mater.*, 2013, **12**, 81.
- 8 J. Zeng, J. Yang, J. Y. Lee and W. Zhou, *J. Phys. Chem. B*, 2006, **110**, 24606.
- 9 S. Guo, L. Wang, S. Dong and E. Wang, *J. Phys. Chem. C*, 2008, **112**, 13510.
- 10 H. A. Esfahani, L. Wang, Y. Nemoto and Y. Yamauchi, *Chem. Mater.*, 2010, **22**, 6310.
- 11 X. Peng, M. C. Schlamp, A. V. Kadavanich and A. P. Alivisatos, *J. Am. Chem. Soc.*, 1997, **119**, 7019.
- 12 S. E. Havas, H. Lee, V. Radmilovic, G. A. Somorjai and P. Yang, *Nat. Mater.*, 2007, **6**, 692.
- 13 B. Lim, J. Wang, P. H. C. Camargo, M. Jiang, M. J. Kim and Y. Xia, *Nano Lett.*, 2008, **8**, 2535.
- 14 X. Duan and C. M. Lieber, *Adv. Mater.*, 2000, **12**, 298.
- 15 Y. Xia, P. Yang, Y. Sun, Y. Wu, B. Mayers, B. Gates, Y. Yin, F. Kim and H. Yan, *Adv. Mater.*, 2003, **15**, 353.
- 16 S. Kan, T. Mokari, E. Rothenberg and U. Banin, *Nat. Mater.*, 2003, **2**, 155.
- 17 R. Agarwal and C. M. Lieber, *Appl. Phys. A*, 2006, **85**, 209.
- 18 R. D. Robinson, B. Sadtler, D. O. Demchenko, C. K. Erdonmez, L. W. Wang and A. P. Alivisatos, *Science*, 2007, **317**, 355.
- 19 M. S. Strano, C. A. Dyke, M. L. Usrey, P. W. Barone, M. J. Allen, H. Shan, C. Kittrell, R. H. Hauge, J. M. Tour and R. E. Smalley, *Science*, 2003, **301**, 1519.
- 20 M. F. L. D. Volder, S. H. Tawfick, R. H. Baughman and A. J. Hart, *Science*, 2013, **339**, 535.
- 21 S. Guo, S. Dong and E. Wang, *J. Phys. Chem. C*, 2008, **112**, 2389.
- 22 S. Sun, G. Zhang, D. Geng, Y. Chen, M. N. Banis, R. Li, M. Cai and X. Sun, *Chem. Eur. J.*, 2010, **16**, 829.
- 23 Y. Lee, J. Kim, D. S. Yun, Y. S. Nam, Y. S. Horn and A. M. Belcher, *Energy Environ. Sci.*, 2012, **5**, 8328.

- 24 N. T. Khi, J. Yoon, H. Kim, S. Lee, B. Kim, H. Baik, S. J. Kwon and K. Lee, *Nanoscale*, 2013, **5**, 5738.
- 25 F. Tao, M. E. Grass, Y. Zhang, D. R. Butcher, J. R. Renzas, Z. Liu, J. Y. Chung, B. S. Mun, M. Salmeron and G. A. Somorjai, *Science*, 2008, **322**, 932.
- 26 F. Abild-Pedersen and M. P. Andersson, *Surf. Sci.*, 2007, **601**, 1747.
- 27 A. Halder and N. Ravishankar, *Adv. Mater.*, 2007, **19**, 1854.
- 28 Y. Kang, X. Ye and C. B. Murray, *Angew. Chem. Int. Ed.*, 2010, **49**, 6156.
- 29 J. Wu, A. Gross and H. Yang, *Nano Lett.*, 2011, **11**, 798.
- 30 B. Wu, N. Zheng and G. Fu, *Chem. Commun.*, 2011, **47**, 1039.
- 31 J. Yoon, N. T. Khi, H. Kim, B. Kim, H. Baik, S. Back, S. Lee, S.-W. Lee, S. J. Kwon and K. Lee, *Chem. Commun.*, 2013, **49**, 573.
- 32 K. S. Cho, D. V. Talapin, W. Gaschler and C. B. Murray, *J. Am. Chem. Soc.*, 2005, **127**, 7140.
- 33 N. Pradhan, H. Xu and X. Peng, *Nano Lett.*, 2006, **6**, 720.
- 34 L. Cademartiri and G. A. Ozin, *Adv. Mater.*, 2009, **21**, 1013.
- 35 Z. Huo, C. K. Tsung, W. Huang, X. Zhang and P. Yang, *Nano Lett.*, 2008, **8**, 2041.
- 36 H. Kim, N. T. Khi, J. Yoon, H. Yang, Y. Chae, H. Baik, H. Lee, J.-H. Sohn, K. Lee, *Chem. Commun.*, 2013, **49**, 2225.
- 37 N. Tian, Z. Y. Zhou, S. G. Sun, Y. Ding and Z. L. Wang, *Science*, 2007, **316**, 732.
- 38 K. Lee, M. Kim and H. Kim, *J. Mater. Chem.*, 2010, **20**, 3791.
- 39 E. P. Lee, Z. Peng, W. Chen, S. Chen, H. Yang and Y. Xia, *ACS Nano*, 2008, **2**, 2167.
- 40 L. Ruan, E. Zhu, Y. Chen, Z. Lin, X. Huang, X. Duan and Y. Huang, *Angew. Chem. Int. Ed.*, 2013, **52**, 12577.
- 41 B. Y. Xia, W. T. Ng, H. B. Wu, X. Wang and X. W. Lou, *Angew. Chem. Int. Ed.*, 2012, **51**, 7213.
- 42 B. Y. Xia, H. B. Wu and X. W. Lou, *Angew. Chem. Int. Ed.*, 2013, **52**, 12337.
- 43 S. W. Lee, S. Chen, J. Suntivich, K. Sasaki, R. R. Adzic, and Y. S. Horn, *J. Phys. Chem. Lett.*, 2010, **1**, 1316.

Table of contents



Ultralong coaxial Au@Pt nanocable prepared by one-pot synthesis exhibits an excellent electrocatalytic activity due to structural features of 1) numerous twinning boundaries and 2) lattice mismatch between core and shell.